2004

Record of Late Pleistocene Glaciation and Deglaciation in the Southern Cascade Range. I. Petrological Evidence from Lacustrine Sediment in Upper Klamath Lake, Southern Oregon

Richard L. Reynolds
US Geological Survey

Joseph G. Rosenbaum
US Geological Survey

Josh Rapp
US Geological Survey

Michael W. Kerwin
US Geological Survey

J. Platt Bradbury
US Geological Survey

See next page for additional authors

Journal of Paleolimnology **31:** 217–233, 2004.
© 2004 *Kluwer Academic Publishers. Printed in the Netherlands.*

Record of late Pleistocene glaciation and deglaciation in the southern Cascade Range. I. Petrological evidence from lacustrine sediment in Upper Klamath Lake, southern Oregon★

Richard L. Reynolds[1,*], Joseph G. Rosenbaum[1], Josh Rapp[1], Michael W. Kerwin[1], J. Platt Bradbury[1], Steven Colman[2] and David Adam[3]
*[1]US Geological Survey, Box 25046, MS 980, Federal Center, Denver, CO 80225, USA; [2]US Geological Survey, 384 Woods Hole Road, Woods Hole, MA 02543, USA; [3]18522 Sentinel Ct., Middletown, CA 95461, USA; *Author for correspondence (e-mail: rreynolds@usgs.gov)*

Received 1 May 2002; accepted in revised form 2 July 2003

Key words: Glacial flour, Lacustrine sediment, Late Pleistocene, Paleoclimate, Sediment magnetism

Abstract

Petrological and textural properties of lacustrine sediments from Upper Klamath Lake, Oregon, reflect changing input volumes of glacial flour and thus reveal a detailed glacial history for the southern Cascade Range between about 37 and 15 ka. Magnetic properties vary as a result of mixing different amounts of the highly magnetic, glacially generated detritus with less magnetic, more weathered detritus derived from unglaciated parts of the large catchment. Evidence that the magnetic properties record glacial flour input is based mainly on the strong correlation between bulk sediment particle size and parameters that measure the magnetite content and magnetic mineral freshness. High magnetization corresponds to relatively fine particle size and lower magnetization to coarser particle size. This relation is not found in the Buck Lake core in a nearby, unglaciated catchment. Angular silt-sized volcanic rock fragments containing unaltered magnetite dominate the magnetic fraction in the late Pleistocene sediments but are absent in younger, low magnetization sediments. The finer grained, highly magnetic sediments contain high proportions of planktic diatoms indicative of cold, oligotrophic limnic conditions. Sediment with lower magnetite content contains populations of diatoms indicative of warmer, eutrophic limnic conditions. During the latter part of oxygen isotope stage 3 (about 37–25 ka), the magnetic properties record millennial-scale variations in glacial-flour content. The input of glacial flour was uniformly high during the Last Glacial Maximum, between about 21 and 16 ka. At about 16 ka, magnetite input, both absolute and relative to hematite, decreased abruptly, reflecting a rapid decline in glacially derived detritus. The decrease in magnetite transport into the lake preceded declines in pollen from both grass and sagebrush. A more gradual decrease in heavy mineral content over this interval records sediment starvation with the growth of marshes at the margins of the lake and dilution of detrital material by biogenic silica and other organic matter.

Introduction

Late Pleistocene sediments from Upper Klamath Lake (Figure 1) are uncomplicated in composition and physical properties compared to sediments in some other coeval lacustrine settings in the western US, such as Pyramid Lake in northwest

★This is the sixth in a series of eight papers published in this special issue, resulting from paleoenvironmental studies in the Upper Klamath Lake Basin. These studies were conducted by the U.S. Geological Survey and its collaborators as part of a paleoclimate research effort called the Correlation of Marine and Terrestrial Records Project. Steven M. Colman served as guest editor of this special issue.

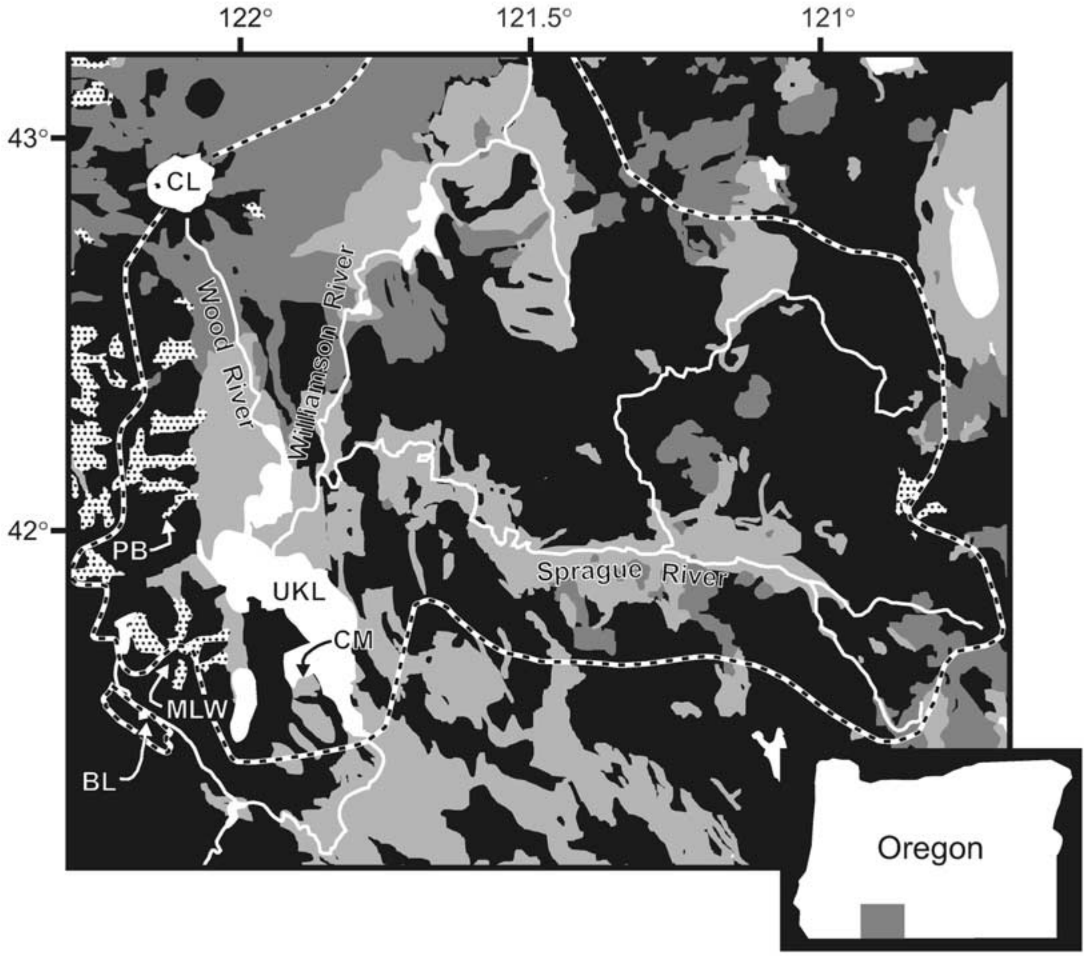

Figure 1. Map showing simplified geology (from Walker and MacLeod 1991) and locations of features in the area of the Upper Klamath Lake (UKL) catchment (dashed line). Buck Lake (BL) and its small (60 km^2) catchment (dashed line around BL) are southwest of the site for core CM2 at Caledonia Marsh (CM). Map patterns: black – basalt and andesite; dark gray – dacite and rhyolite; light gray – Quaternary and Tertiary sediments and Quaternary alluvium; stippled – glacial deposits. Crater Lake – CL; Pelican Butte – PB; Mountain Lakes Wilderness – MLW.

Nevada (Benson and Thompson 1987), Ovens Lake in southern California (Benson et al. 1996; Bischoff et al. 1997; Smith et al. 1997), and Great Salt Lake in northern Utah (Oviatt 1997). The relative simplicity of the sediments from Upper Klamath Lake results from a combination of geological and limnological characteristics of the lake and its catchment. First, production of biological sediment within the late Pleistocene lake was uniform and low. Second, the lake drained continuously providing an uninterrupted record of sedimentation. Third, authigenic minerals, such as carbonate or iron sulfide minerals, were not precipitated. Fourth, there is no evidence for significant shifts in lake level, climatic or otherwise, over the past ca. 40 ka years that might have affected sediment transport and deposition at a given core site (Bradbury et al. 2004a, b – this issue). This characteristic also contrasts Upper Klamath Lake with nearby Tule Lake (Bradbury 1991). Finally, the bedrock geology of the large (about 9650 km^2) catchment is dominated by mafic volcanic rocks, so that sediments derived from them are mostly uniform in mineral and chemical composition.

The late Pleistocene setting for Upper Klamath Lake thus provides the opportunity to interpret petrological and textural properties of the lacustrine sediments in a core from Caledonia Marsh (core CM2; Figure 1) in terms of changes in catchment processes (e.g., weathering and sediment transport) that might be caused by changes in climate. As described below, variations in these properties correspond closely to changes in paleoenvironmental conditions reconstructed from pollen and diatom records. Pollen analysis (Adam et al. 1995) documents a major shift from cold and dry to warmer and mostly wetter conditions from the late Pleistocene to early Holocene. Detailed analysis of diatoms elucidates abrupt paleolimnological changes on scales of a few centuries to millennia that reflect varying seasonal inputs of nutrients under changing conditions of lake circulation, ice cover, and wind stress (Bradbury et al. 2004a, b – this issue).

For this study, sediment magnetic properties are used to quantify petrological changes in these lithogenic sediments. Complemented with textural and geochemical data, the magnetic results record varying input volumes of glacial flour into the lake during oxygen isotope stages (OIS) 2 and 3. This paper thus establishes the physical link between climate (glaciation) and climate proxies (sediment magnetic properties and bulk sediment particle-size). This link is the foundation for a companion paper (Rosenbaum and Reynolds 2004a – this issue) that calculates the flux of glacial flour at Caledonia Marsh.

Setting

Upper Klamath Lake lies in the northern part of Klamath basin (southern Oregon), east of the crest of the southern Cascade Range and about 200 km from the Pacific Ocean. Bradbury et al. (2004a, b – this issue) present details about the limnological and ecological setting before and after hydraulic manipulation beginning in 1911. Bacon et al. (1999) and Colman et al. (2000) discuss the neotectonism of the area and new evidence for recurrent faulting of the lake sediments during the Holocene.

Bedrock in the catchment is mostly basalt and basaltic andesite (Figure 1). Lesser amounts of more silicic volcanic rocks (dacite, rhyodacite, and rhyolite) occur with basalt in the Devils Garden lava field east of Klamath Lake (McKee et al. 1983). To the north of Upper Klamath Lake, the eruptive evolution of Mount Mazama, a complex of volcanic shields and stratovolcanoes, culminated in collapse of Crater Lake caldera at 7.55 ka (Bacon 1983). Rocks associated with this eruptive sequence include a range of compositions from basalt to rhyolite, including rhyodacite tuff ejected during caldera formation. Late Miocene to Holocene fluvial and lacustrine deposits also occupy the catchment (Sherrod 1991).

The catchment was partly glaciated several times during the Quaternary (Figure 1). Although drainages directly into Caledonia Marsh and Howard Bay were not glaciated, repeated advances of alpine glaciers in valleys elsewhere on the eastern side of the Cascadian crest produced large morainal deposits nearly to the shoreline of the present-day lake (Smith 1988). Glaciers also mantled Mt. Mazama (centered on present-day Crater Lake; Bacon 1983). Maps and analyses of glacial deposits by Carver (1972) document extensive glacial cover in the catchment during the Last Glacial Maximum (Rosenbaum and Reynolds 2004a – this issue). An ice cap formed along the range crest and fed valley glaciers toward the lake to elevations below 1500 m. Extensive alpine glaciers also formed in the catchment, some on the high peaks of the Mountain Lakes area, and others on lower features, such as Pelican Butte (elevation 2450 m) (Figure 1). In contrast, the catchment for nearby Buck Lake (Figure 1) was never glaciated. The vastly different textural properties between sediments from Upper Klamath Lake and Buck Lake, described herein, provide critical evidence bearing on magnetic record of glaciation in the Upper Klamath Lake catchment.

Core age and lithology

Core CM2 was taken from a road berm built in 1916 to separate Caledonia Marsh from Howard Bay in the southern part of the lake. Descriptions of coring, as well as the age control, lithology, and geochemistry of the core are given by Colman et al. (2004). Here we summarize aspects of these descriptions (with ages in calendar years) that are essential background for this paper. The age model for the 12.86-m core is controlled by tephra layers and 17 radiocarbon dates (Colman et al. 2004). Intervals of tephra, including the bottom of the core (sediment below 1190 cm; older than 37.5 ka),

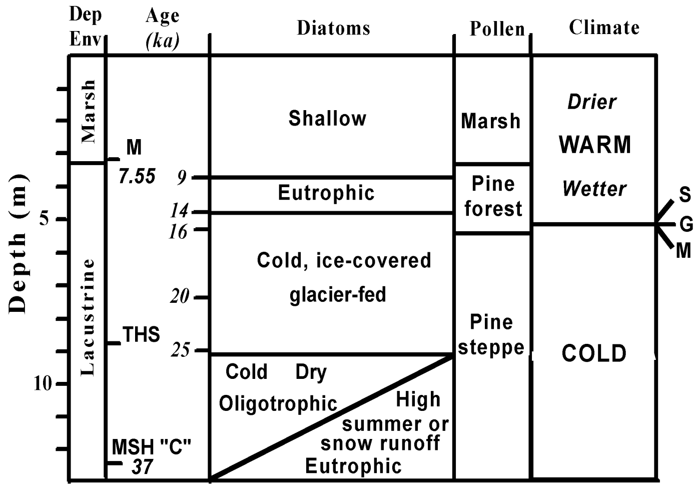

Figure 2. Summary of the evolution of the lake-marsh setting recorded in core CM2 from Caledonia Marsh. Dep Env – generalized depositional environment. Tephra layers are denoted as M (Mazama), THS (Trego Hot Springs), and MSH 'C' (Mt. St. Helens 'C'). Upward declines in certain types of pollen are denoted by S for sagebrush and by G for grass. M marks the onset of abrupt upward decrease in MS and S parameter values.

are discounted from our paleoenvironmental analysis, because the tephra affects magnetic properties and particle-size results.

A major sedimentological change is visually and chemically apparent at about 500 cm in the core (about 14.8 ka). Sediment below is medium-gray clayey silt, whereas sediment above is olive gyttja. This lithological change corresponds to upward increases in organic carbon and in biogenic silica from diatoms. Biogenic silica increases strongly between 500 and 400 cm and dominates sediment above about 400 cm (10.1 ka). Organic carbon is low (<1%) below 500 cm, with systematic increases upward: 1–4% to 395 cm (10 ka), 4–10% to 330 cm (7.9 ka), and 10–50% to about 170 cm (about 5.5 ka). Above 170-cm depth, organic carbon values diminish below about 10%. Overall, the sediment contains uniformly small contents of sand-size lithogenic particles (<20%), with the exception of the tephra beds near the base of the core. XRD analyses on bulk sediment reveal dominant feldspar, with lesser augite and minor quartz. Smectite is the major clay mineral, and minor kaolinite is also present.

Evolution of the lake and climate history

Variations in pollen, diatoms, and organic matter reveal how Upper Klamath Lake evolved in response to climatic change during OIS stages 1, 2, and most of stage 3. The evolution of the lake-marsh setting is summarized in Figure 2. Between about 38 and 16 ka, changes in lake conditions are documented by variations in planktic diatom populations (Bradbury et al. 2004b – this issue), three species of which are discussed in this paper. Two of these species are cold-water diatoms: *Aulacoseira islandica* and *A. subarctica*. *A. subarctica*, which blooms in the spring or fall, fluctuates abruptly in the deeper part of the core, commonly in sympathy with lesser amounts of *A. islandica* and antithetically with *A. ambigua*. *A. ambigua* is a warmer water, summer-blooming diatom that reflects either increased precipitation in the summer or a snow-melt season extending into summer. Taken together, the diatom populations indicate strong millennial-scale fluctuations between oligotrophic (*A. subarctica*) and eutrophic (*A. ambigua*) lake conditions over the depth interval 1200–850 cm (about 38–23 ka) (Bradbury et al. 2004b – this issue). Lake conditions evolved into generally very cold limnic conditions and long periods of ice cover over the interval 800–540 cm (about 21–16.3 ka; corresponding largely to much of the Last Glacial Maximum). The emergence and abundance of *A. islandica* in this interval documents more turbid conditions than represented by *A. subarctica* (Bradbury et al. 2004b – this issue).

The pollen record (Adam et al. 1995) reveals a cold, dry, pine-steppe environment, as indicated from sagebrush, grass, and variations in pine (*Pinus*) from the core bottom to about 510 cm (15.3 ka). Over this interval, fluctuations in *A. ambigua* are not correlative with fluctuations in *Pinus* percentages. Increased warmth and moisture led to a pine forest environment, marked initially by a decline in grass (beginning at about 510 cm) and then by a decline in sagebrush (Figure 2). After about 7 ka (depths above 265 cm), warmer and drier conditions that are indicated by a decline in pine and an increase in Cyperaceae (sedges and bullrushes), led to the extensive development of marshes around much of the lake. Since then, the lake has been starved of fluvial sediments, leading to lake sediments that consist mainly of diatoms and organic matter (Bradbury et al. 2004b – this issue).

Methods

Core CM2 was sampled for sediment magnetic measurements by pushing oriented plastic cubes (3.2 cm^3) into soft sediment at a 5-cm spacing. Magnetic properties were measured on these wet sediments; the samples were later dried and weighed, and remeasured for magnetic susceptibility (MS). Sediment representing an interval of 2–3 cm centered on the middle of the plastic cube was used for geochemical and other analyses. Analyses for particle size and biogenic silica were done on samples collected initially in the plastic cubes. Combined magnetic (Thompson and Oldfield 1986; Verosub and Roberts 1995) and petrographic methods were used to determine the types, amounts, and grain sizes of magnetic minerals. The identification of magnetic-mineral type was primarily done with reflected-light microscopy. The grains were prepared in polished grain mounts after they had been isolated from the bulk sediment in a magnetic separator similar to that described by Petersen et al. (1986). The identification of magnetic minerals was also made from the measurement of Curie temperatures using thermomagnetic analysis and from X-ray diffraction analysis of magnetic-mineral separates. Common magnetic minerals belong to two groups: low-coercivity ferrimagnetic oxides (e.g., strongly magnetic magnetite, including titano-

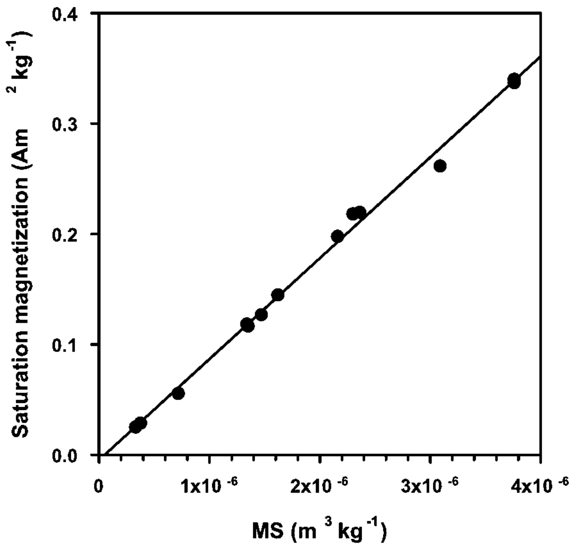

Figure 3. Plot of magnetic susceptibility (MS) against saturation magnetization, measured in a vibrating sample magnetometer, indicating that MS is a measure of magnetite. Regression line fit, $r^2 = 0.99$.

magnetite, and maghemite) and high-coercivity ferric oxide minerals (e.g., hematite), We refer to these groups more simply as magnetite and hematite, because, as discussed below, titanomagnetite and hematite are the dominant Fe–Ti oxide minerals in the lake sediment.

The abundance of magnetite was determined from MS measurements in a 0.1 milliTesla induction at frequencies of 600 Hz, using a susceptometer with sensitivity better than 2×10^{-10} m^3 kg^{-1}. For a subset of samples, the strong correlation of MS with saturation magnetization (measured using a vibrating sample magnetometer; Figure 3) confirms that MS is an excellent measure of magnetite content. A measure of the quantity of magnetite sufficiently large (greater than about 30 nm) to carry remanence is isothermal remanent magnetization (IRM), the magnetization acquired by a sample after exposure to a strong magnetic field. Remanent magnetization was measured using a 90-Hz spinner magnetometer with a sensitivity of about 10^{-5} Am^{-1}. Hard IRM (HIRM) is a measure of hematite. Whereas low-coercivity magnetite saturates magnetically below applied fields of 0.3 Tesla (T), hematite continues to acquire IRM above 0.3 T. In this study, HIRM is calculated: $(IRM_{1.2T}-IRM_{0.3T})/2$. The ratio, $IRM_{0.3T}/IRM_{1.2T}$ thus is a measure of the proportion of magnetite to all magnetic iron oxides. When values of this ratio, called the *S* parameter, are high, the iron oxide population is dominated by magnetite (a maximum value of 1); decreasing values indicate increasing proportions of hematite. Information about the magnetic grain size (magnetic domain state) of magnetite was obtained from the concentration–independent ratio of anhysteretic remanent magnetization (ARM) to MS which is sensitive to single domain and small pseudo-single domain grain sizes. Increasing ARM/MS values indicate decreasing magnetic grain size. ARM was imparted in a decaying alternating field with a peak induction of 100 mT and a D.C. bias of 0.1 mT.

Energy-dispersive X-ray fluorescence (XRF) analysis for 14 elements was done on 70 samples (Rosenbaum et al. 1997). Ti, Zr, and Fe are useful tracers of detrital heavy minerals. Ti and Zr are chemically immobile (Winchester and Floyd 1977) under most post-depositional lacustrine chemical conditions and thus provide a measure of initial abundance of certain heavy minerals, such as Fe–Ti oxides (e.g., titanomagnetite and ilmenite) and zircon. Moreover, Zr/Ti is a useful parameter by which to gauge possible changes in provenance (Muhs 1983; Muhs et al. 1990; Kerwin 1996; Reynolds et al. 2001). For example, Zr/Ti increases over a range in rock types from mafic (e.g., basalt) to more silicic (e.g., rhyodacite). Finally, because Ti and Fe commonly vary together, their ratio enables us to evaluate the possible loss of Fe via post-depositional magnetite dissolution, especially when used in conjunction with petrographic analysis (Rosenbaum et al. 1996).

Biogenic silica was determined by the methods for opal extraction described by Mortlach and Froelich (1989). Opal contents were corrected for Al_2O_3 content measured in the extraction solute to account for silica liberated from the dissolution of clay. The correction assumes 2% clay-bound silica for 1% of Al_2O_3 on the basis of silica content in common clays such as smectite. The corrected opal values in the Caledonia Marsh sediments are considered a measure of biogenic silica, because smectite is the dominant clay mineral. Particle size was measured using a laser-light scattering method capable of measuring particles between 0.03 and 1000 μm. All samples (70 from Caledonia marsh, 39 from Buck Lake) were treated first to remove

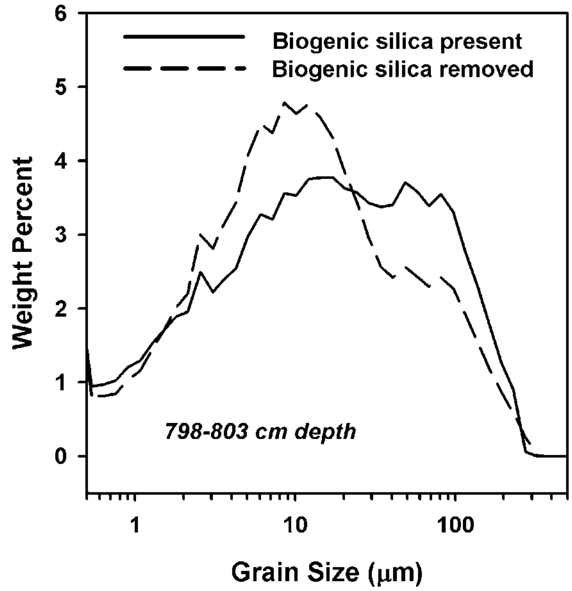

Figure 4. Results of particle-size analyses before and after chemical treatment to remove biogenic silica.

carbonate, organic matter, and biogenic silica. In nine samples from Caledonia Marsh we compared bulk sediment grain size before and after the different treatments. For each sample, grain size decreased substantially after the dissolution of diatoms (Figure 4).

Magnetic property variations

Amounts, relative contents, and grain size of iron oxide minerals vary greatly through core CM2 (Figure 5). The largest magnetic variations correspond to vastly different paleoenvironmental conditions interpreted from the pollen and diatom analyses. High concentrations of magnetite (high MS values) and hematite (high HIRM values) characterize the cold climate part of the record from the bottom of the core to about 530 cm; in contrast, magnetite and hematite contents are low in the warm climate zone (above 500 cm depth). Magnetite content drops abruptly between 530 and 490 cm and then gradually diminishes to about 360 cm. Changes in hematite content do not exactly track these changes in magnetite. Rather, hematite declines more gradually, beginning at about 520–360 cm, the depth above which marsh deposits dominate. Hematite varies in generally

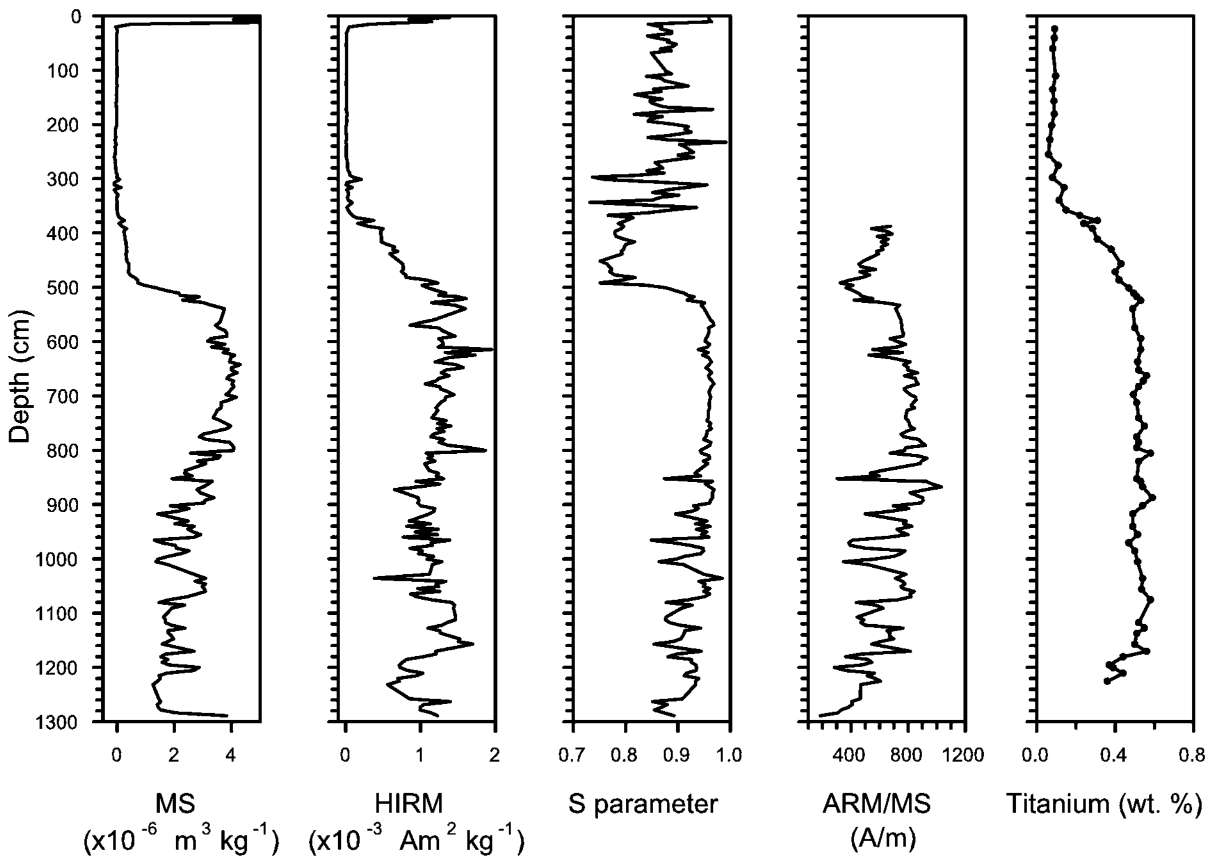

Figure 5. Depth plots of magnetic properties and titanium. MS, magnetic susceptibility, a measure of magnetite content. HIRM, 'hard' isothermal remanent magnetization, a measure of hematite content. *S* parameter, a measure of relative abundance of magnetite and hematite, higher values indicating relatively more magnetite. ARM/MS, ratio of anhysteretic magnetization to MS, a measure of magnetic grain size of magnetite, larger values indicating smaller magnetic grain size (not shown above 380 cm because of low, commonly negative, MS values).

low amounts through the marsh sequence. Higher contents of both magnetite and hematite in the upper 7 cm of the core are caused by construction material in the road berm intersected in the core.

The cold climate zone is also characterized by high content of magnetite relative to hematite (high *S* parameter values; Figures 5 and 6). The abrupt shift to higher relative hematite content (decreasing *S*) above 530 cm depth closely tracks the decline in absolute magnetite content (Figure 6). High relative hematite content (low *S* values) characterizes the interval 360–490 cm; the variable *S* values in the marsh sediments are not interpreted here with respect to environmental changes because of the extremely low amount of lithic sediment. Excluding marsh sediment, magnetic grain size of magnetite similarly corresponds to climatic zonation. Overall, finer magnetic grain size (relatively high values of ARM/MS) characterizes the cold-climate zone, whereas coarser magnetic grain size abruptly marks the bottom of the warm-climate zone.

Magnetite content and magnetic grain size vary strongly even within the cold climate sediments. Between 1190 and 530 cm, MS values range from about 1.3×10^{-6} to more than 4×10^{-6} m^3 kg^{-1} indicating changes in magnetite content by a factor of about 3. Magnetite content increases upward, becoming uniformly highest in the interval 700–570 cm. Below this interval, the MS profile defines prominent fluctuations. Zones of high magnetite content (high MS) correspond tightly with zones having high content of magnetite relative to hematite (high *S* values; Figure 6) and having comparatively small magnetic grain size (high ARM/MS).

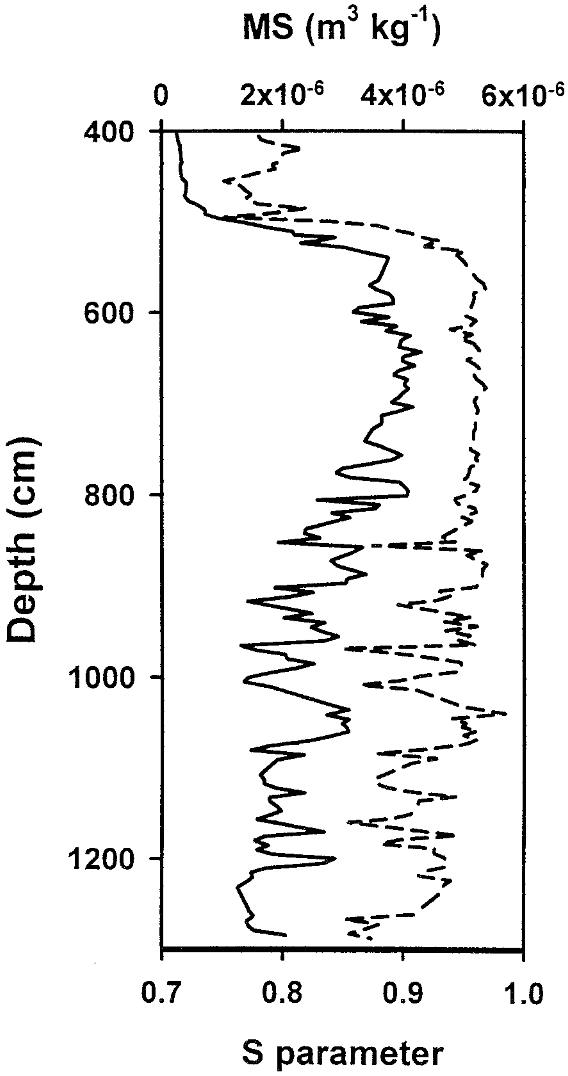

Figure 6. Depth plot of MS (solid) and *S* parameter (dashed) showing close correspondence between high content of magnetite and a high degree of freshness (lack of alteration of magnetite to hematite) of the iron oxide suite.

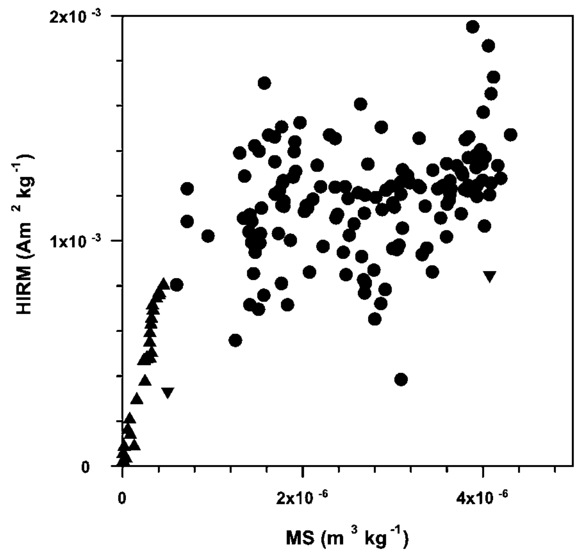

Figure 7. Plot of MS against HIRM. Triangles represent samples from depths above 480 cm; the two inverted triangles are from sediment disturbed in the construction of the berm at the top of the core. Solid circles represent samples from depths below 480 cm.

A thick zone (about 820–570 cm) of uniformly high *S* values and nearly constant ARM/MS encompasses and extends below the interval of uniformly high magnetite content.

Although hematite content varies strongly, as does magnetite, there are some differences between magnetite and hematite distributions. First, hematite content shows no trend between 1180 and 540 cm, an interval over which magnetite increases upward to reach highest contents in the Last Glacial Maximum interval. Second, the HIRM profile lacks prominent swings over the interval between 1080 and 740 cm. Finally, low-frequency shifts in magnetite and hematite contents do not closely correspond. This lack of tight correspondence between magnetite and hematite contents over both the cold-climate zone (>530 cm depth) and pre-marsh warm-climate zone (530 to 360 cm) is seen in a plot of MS *versus* HIRM (Figure 7).

Causes for magnetic property variations

The very close correspondence among magnetic properties and paleoenvironmental indicators may result from one or more factors. Possible factors include biogenic dilution of magnetic signals, post-depositional alteration of magnetic iron-titanium oxide minerals, post-depositional growth of magnetic minerals, and climatically controlled catchment processes of weathering and sediment transport. To identify the responsible factors, we compared magnetic and geochemical data, examined the magnetic mineralogy in detail, and measured bulk sediment particle-size distributions that might provide clues to catchment processes.

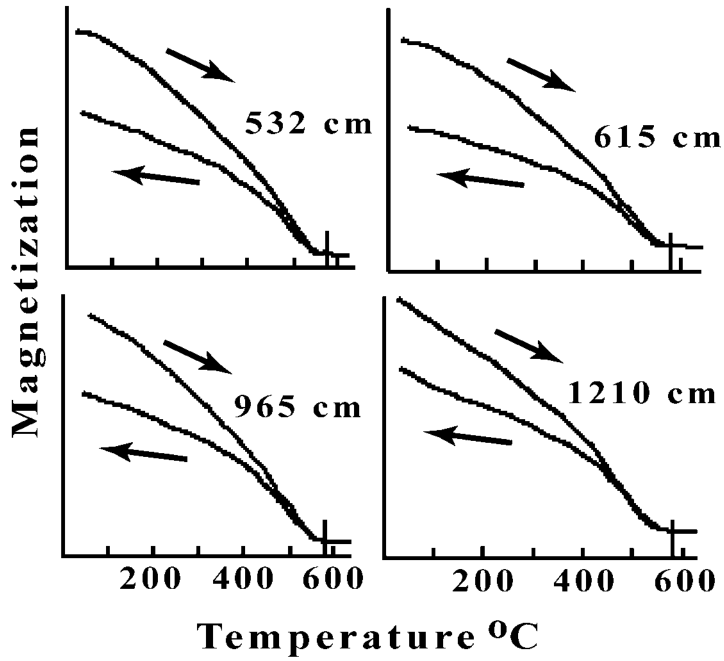

Figure 8. Examples of saturation magnetization *versus* temperature curves determined for magnetic separates from core CM2. Arrow to the right indicates heating curve; arrow to the left indicates cooling curve. Magnetization is lost over a broad range in temperature (typically from 500 to 560 °C), indicating a range of Ti contents in titanomagnetite. No sample showed a discrete Curie temperature of pure magnetite at 580 °C that would be expected for bacteriogenic (Ti-free) magnetite (e.g., Lovley et al. 1987; Snowball 1994).

Biogenic dilution

Within the cold-climate sediments, the biogenic fraction (organic carbon and biogenic silica) is low and nearly constant (biogenic silica averages 14.4%; one sigma, 1.7%), but it increases gradually to >80% between 510 and 340 cm. In this depth interval, this increase closely mirrors the decline in hematite (Figure 5). The decreases in Ti, Zr, Fe, and hematite shallower than 510 cm are evidence for biogenic dilution of lithogenic components in this part of the core. However, biogenic dilution cannot account for the earlier sharp decrease in magnetite beginning at about 530 cm, nor for the fluctuations in magnetic properties at greater depths, as indicated by the low and nearly constant biogenic silica, the absence of organic carbon, and constant Ti content. In the deep part of the core, the different patterns of hematite and magnetite contents (Figures 5 and 7) further argue against biogenic dilution as a cause of these magnetic property variations.

Evidence from iron oxide mineralogy

Combined XRD, thermomagnetic (Figure 8), and petrographic analyses confirm detrital titanomagnetite and hematite as the sources of the magnetic record of climate change. Magnetic oxides are found as grains of titanomagnetite and specular hematite, which is typically associated with other Fe oxides, such as titanomagnetite and pseudobrookite. Magnetic oxides are also found as particles in volcanic rock fragments, two types of which are observed: (1) chemically unaltered (fresh) fragments that contain small, typically 1–10 μm, unaltered magnetic oxides, and (2) altered fragments in which oxidation has produced a reddened matrix caused by fine-grained hematite. Discrete magnetic oxide particles in the latter type of fragment are usually partly to completely oxidized.

The occurrence and texture of magnetic oxides differ greatly in the lake sediment corresponding to the different magnetic and climatic zones. In the high-MS sediment below 500-cm depth, the

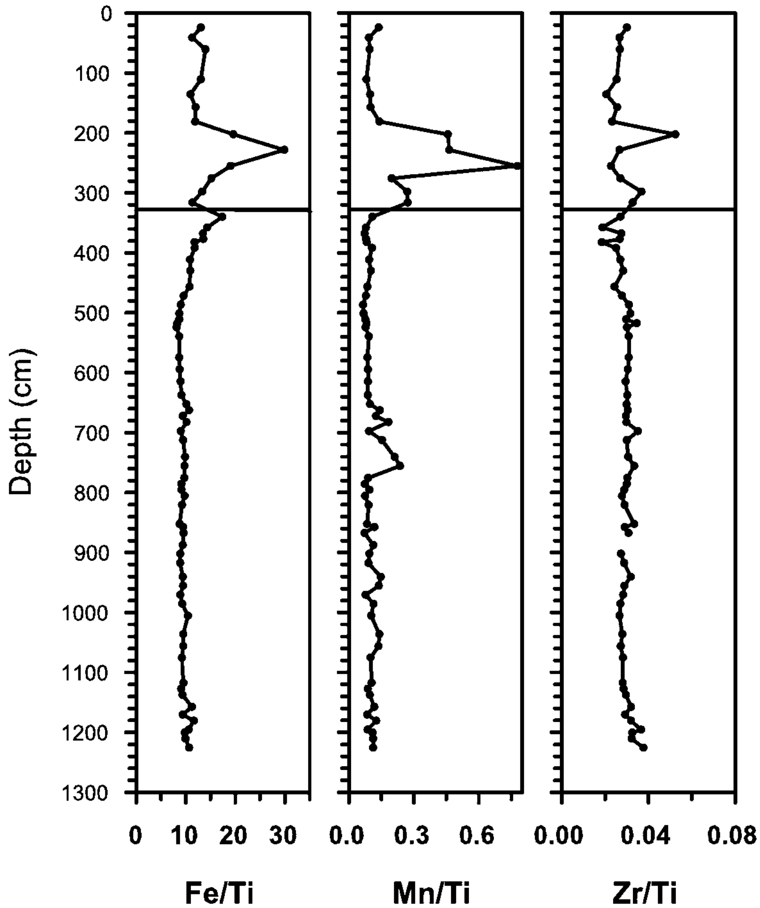

Figure 9. Depth plots of elemental ratios. The constant Fe/Ti and Mn/Ti ratios indicate an absence of post-depositional alteration. The constant Zr/Ti from 1200 to 400 cm indicates unchanging sediment sources.

individual magnetic oxide particles and unaltered volcanic rock fragments are angular and typically <40 μm in size. Many such oxide particles and rock fragments are noteworthy for their very small (<10 μm) size in the fine silt range. Some oxide particles and oxidized rock fragments in the high-MS sediments are relatively large (>40 μm). In the low MS sediment shallower than about 500 cm, the magnetic particles and rock fragments that contain them overall are larger than those in deeper sediment, ranging typically in the medium silt to fine sand size (20–100 μm). Two other differences stand out. First, many such grains in the low-MS sediments are rounded, in contrast to the fine-grained angular particles that characterize deeper sediment. Second, these low-MS sediments lack unaltered mafic rock fragments containing small, fresh titanomagnetite.

Alteration

In these sediments, possible post-depositional dissolution of Fe–Ti oxides can be discounted by comparing the distributions of chemically immobile Ti with those of Fe and Mn, which may be relatively mobile under reducing conditions (Rosenbaum et al. 1996). Below 400 cm, nearly constant ratios of Fe/Ti, Mn/Ti, and Zr/Ti (Figure 9) strongly suggest nearly uniform sediment provenance, combined with a lack of Fe–Ti oxide dissolution. The tight, linear plot of Ti *versus* Fe (Figure 10) not only illustrates this constant ratio, but also shows a positive intercept on the Fe axis, consistent with a lack of dissolution and Fe mobility (see Rosenbaum et al. 1996). Moreover, there was no evidence from petrographic or magnetic property results for magnetic

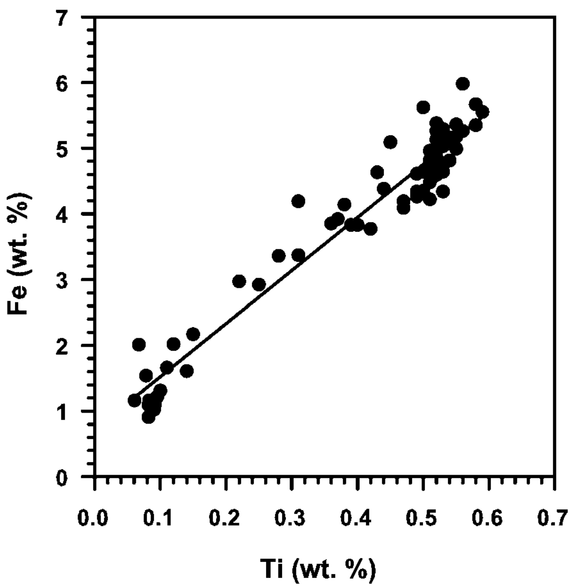

Figure 10. Plot of iron against titanium. Regression line fit, $r^2 = 0.94$.

greigite or nonmagnetic pyrite that could affect the magnetic record (see Snowball and Thompson 1990; Roberts et al. 1996; Reynolds et al. 1999).

Catchment processes recorded by OIS 2 and 3 sediments

In the absence of biogenic dilution and post-depositional alteration, magnetic property variations in the cold-climate zone (corresponding to OIS 2 and most of 3) must be related to changing conditions of weathering, erosion, and sediment transport. Two likely causes can be considered: (1) varying runoff from glaciers that delivered abundant, fresh magnetite in glacial flour to the lake sediment; and (2) changes in peak runoff in streams to produce fresh rock fragments via breakage of stream cobbles. Other possible explanations are unsupported by magnetic and geochemical results. Varying concentrations of heavy minerals cannot account for the magnetic property variations, because Ti is nearly constant in the Pleistocene sediments. The presence of wind-reworked Pliocene diatoms, such as *Cyclotella*, in OIS 2 and 3 sediments (Bradbury et al. 2004b – this issue), raised the possibility that the fresh magnetite responsible for the sharp spikes in MS and S values might similarly be transported under high-wind conditions. Such a possibility can be rejected, because MS variations are out-of-phase with *Cyclotella* content.

It is not possible to distinguish between the possibilities of glacial activity and peak runoff, solely on the basis of the geochemical and magnetic data. As an example, the nearby basaltic catchment of Buck Lake (Figure 1) is unglaciated and magnetic property variations in middle Pleistocene lacustrine sediment there (Rosenbaum et al. 1996) are in many ways similar to those observed at Caledonia Marsh. In a core from Buck Lake where paleoclimate was characterized from pollen studies, high magnetite content, both absolute (high MS) and relative to hematite (high S ratio), characterize cold-climate sediments, whereas low absolute and relative magnetite contents characterize warm-climate sediments. (The magnetic record of climate change at Buck Lake was interpreted by Rosenbaum et al. (1996) to reflect climatically controlled variations in peak runoff.) Thus, magnetic properties by themselves are not diagnostic for glacial flour in the Caledonia Marsh core. To test whether changes in glacial flour input are responsible for magnetic property variations at Caledonia Marsh, we compared bulk sediment particle size in 70 samples (506–1283 cm; Rosenbaum et al. 1997) from core CM2 and in 39 samples from a cold-climate zone in the Buck Lake core. In the glaciated catchment for Upper Klamath Lake, we anticipated that glacial flour would have smaller particle size than sediment produced via breakage of cobbles in unglaciated drainages (see Drewry 1986, pp. 85, 99–100, 117–118).

In the Caledonia Marsh core (500–1230 cm), high magnetite content corresponds to fine particle size, and relatively low magnetite content corresponds to coarser particle size (Figure 11A). Similarly, high proportions of fresh magnetite (high S values) characterize relatively fine-grained sediment (Figure 11B). Only a few samples are not covered by these observations. A magnetite-rich sample in the zone of uniformly high MS at 625 cm is relatively coarse grained. This sample, though, has a slightly elevated 'weathered' component indicated by a small decrease in S value, so that S parameter and phi mean size track closely in this zone. Another short interval at about 1200–1210 cm is characterized by relatively high magnetite content, coarse particle size, and abundant glass shards, and it thus represents reworked

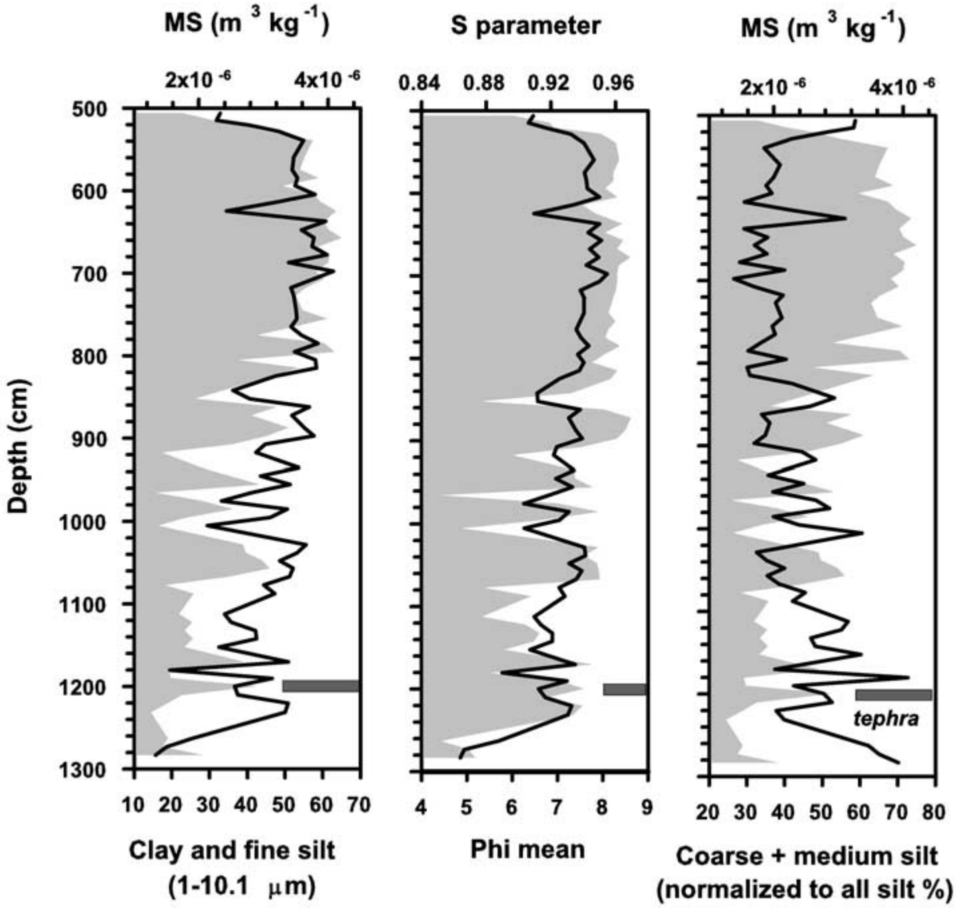

Figure 11. Depth plots of magnetic susceptibility (MS) and *S* parameter (shaded) shown with particle-size results for Caledonia Marsh core. Relations between particle size and magnetic properties are compared using a coarse clay-plus-fine silt component (1–10.1 μm), the medium-plus-coarse silt component (10.1–63 μm) normalized to all silt, and the mean phi size.

tephra (Sarna-Wojcicki, written commun., 1999). Through the Pleistocene sediments, magnetite content clearly varies antithetically with the medium and coarse silt fraction (Figure 11C). As this coarse silt fraction decreases up core, magnetite content increases. Below 800 cm depth, shifts to low magnetite content correspond to abrupt increases in coarse-plus-medium silt.

The close correspondence between high content of magnetite and fine grained sediment found in the Caledonia Marsh sediments core is not found in the Buck Lake sediments, which lack a consistent pattern between magnetic properties and bulk particle size. In many samples from Buck Lake, low magnetite content is associated with high content of clay-plus-fine silt (Figure 12A). Moreover, *S* values are much lower (high relative hematite abundance) than in the Caledonia Marsh core and, for most samples, lack a close correspondence with mean particle size (Figure 12B). Finally, magnetite content varies without clear relation to the medium and coarse silt fraction (Figure 12C).

The contrasting pattern between the sediments in the Caledonia Marsh and Buck Lake cores is illustrated in a plot of MS *versus* clay-plus-fine silt (Figure 13). In the Caledonia Marsh sediments, magnetite content increases with increasing content of fine particles, but no such relation is evident in the Buck Lake sediments. Related clues to understanding the climatic signal in core CM2 stem from a study of catchment rocks and sediments under current conditions of weathering and sediment transport (Rosenbaum and Reynolds 2004b – this

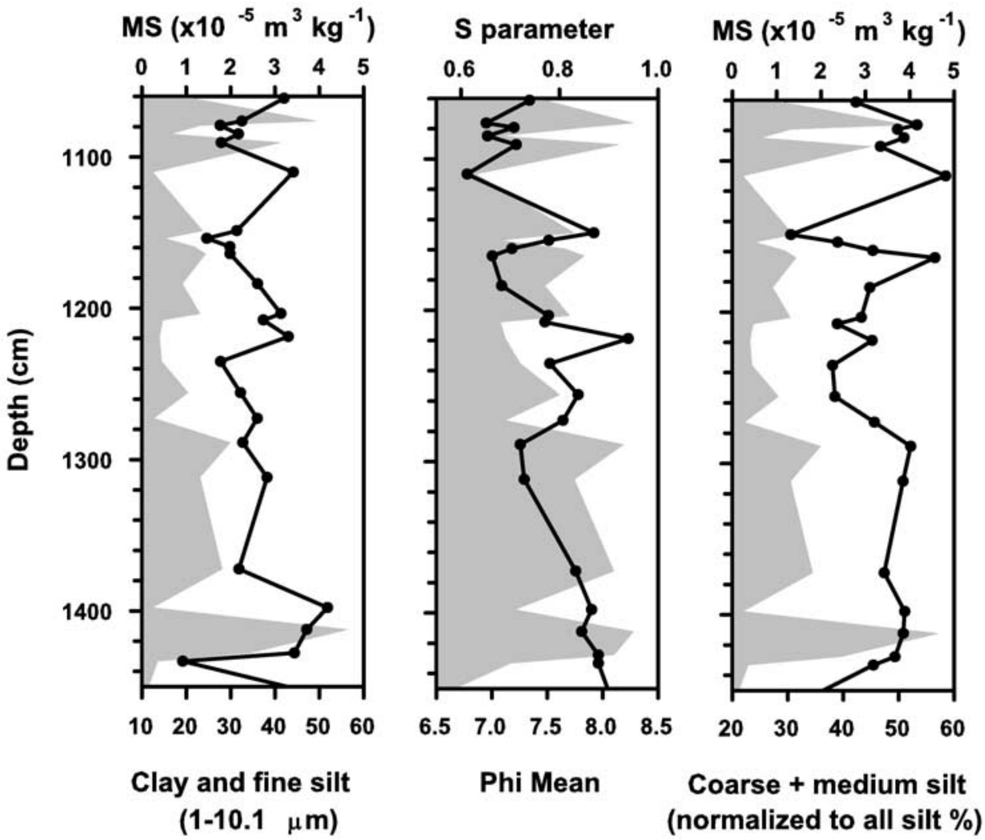

Figure 12. Depth plots of magnetic susceptibility (MS) and *S* parameter (shaded) shown with particle-size results for Buck Lake core.

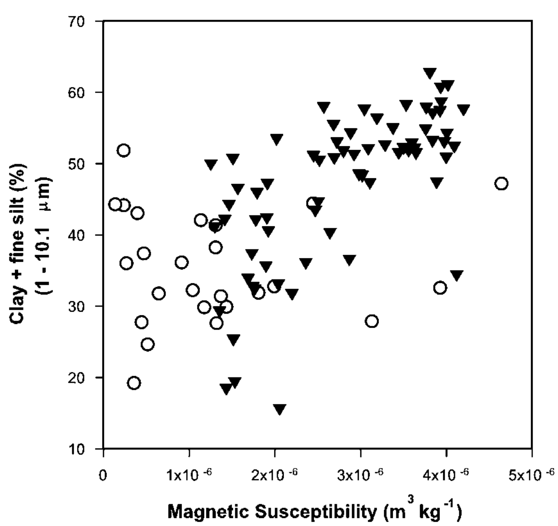

Figure 13. Plot of magnetic susceptibility (MS) against the 1–10 μm fraction (in weight percent). Inverted triangles represent samples from depths between 504 and 1283 cm (regression line $r^2 = 0.44$) from Caledonia Marsh core CM2. Open symbols are from sediments in the Buck Lake core.

issue). Sized sediment fractions separated from today's stream and overbank deposits have vastly different states of 'magnetic freshness' (*S* parameter values) (Figure 14). Fine silt-plus-clay is the most highly weathered fraction (lowest average *S*), whereas increasing freshness (increasing *S*, higher relative magnetite content) corresponds to coarser sediment size. These relations are opposite to those found below the 530-cm depth in core CM2. This contrast indicates that weathering and erosion in today's catchment are vastly different from weathering and erosion that produced fine-grained sediment between 37 and 16 ka.

Comparison of petrological proxies to biological proxies

Comparison among the biological and petrological proxies provides insights into the manner and timing of the response of the lake-catchment

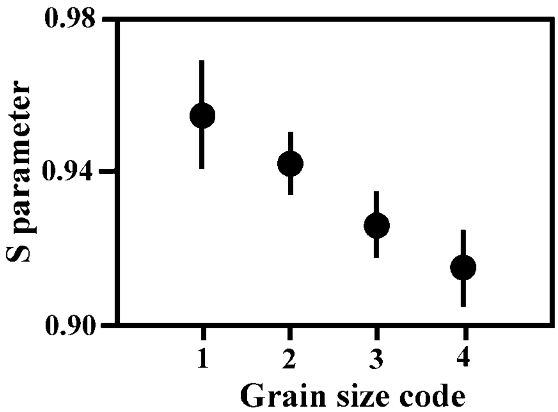

Figure 14. Plot of *S* parameter against grain size classes for samples from the catchment of Upper Klamath Lake. (1) pebbles, n (number of samples) = 59; (2) coarse sand and granules, $n = 73$; (3) fine and medium sand, $n = 74$; (4) silt, $n = 74$. High *S* parameter values (samples dominated by fresh magnetite) characterize the coarser particles. The greatest degree of oxidative alteration of magnetite to hematite has occurred in fine fractions. In contrast, fresh magnetite characterizes the fine silt and clay fractions in the Late Pleistocene sediments of the Caledonia Marsh core.

system to climate change. Major changes in magnetite content and freshness, which represent glacial flour, slightly precede the transition from cold to warm as indicated by changes in pollen, reflecting a lag in vegetation response to deglacial conditions (see Prentice 1986; Webb 1986). For example, the upward decreases in iron oxide contents (beginning about 530 cm, 16 ka) precede the decline in grass pollen (beginning about 510 cm; 15.3 ka) and sagebrush pollen (beginning at 480 cm, 13.9 ka) (Figures 2 and 15). Content of magnetite similarly decreases before the increase in the biogenic fraction (Rosenbaum and Reynolds 2004a – this issue; see Figure 3 in Bradbury et al. 2004b – this issue).

Some important biological and petrological changes occurred simultaneously. The changes in magnetite content, both absolute (MS) and relative to hematite (*S* parameter), in the cold-climate zone show a remarkable correspondence to variations in the three species of *Aulacoseira* in that zone (Figure 15). High contents of fresh magnetite (high MS and *S* values) correspond to large populations of the cold-water diatoms, *A. subarctica* and *A. islandica.* Over the interval about 900–1190 cm (about 25–37.5 ka; most of OIS 3), abundant magnetite is associated with large numbers of *A. subarctica.* Over the Last Glacial Maximum interval above, abundant magnetite is associated with large numbers of *A. islandica*, which replaced *A. subarctica* as the dominant cold-water form. Conversely, lower amounts of magnetite along with relative increases in hematite (lower MS and *S* values) correspond closely to large numbers of *A. ambigua.* The close correspondence between abundant magnetite and *A. islandica* forms a link between high glacial flour discharge and cold turbid water. These relations attest to a very tight linkage between physical processes in the catchment and a coupled biological response in the lake over thousands of years. The rapid response of diatoms to changes in lake conditions is well understood (Stoermer and Smol 1999). The influence of external factors, over thousands of years, on these types of biologic changes is unusually well established in core CM2.

The magnetic record of deglaciation, however, does not exactly track changes in the three species of *Aulacoseira.* The abrupt decline in glacial flour input matches closely with the abrupt decline in *A. islandica*, but glacial flour continued to enter the lake even as younger populations of *A. subarctica* and *A. ambigua* quickly expanded and then disappeared (Figure 15). Receding glaciers thus produced glacial flour, while water temperature increased and early spring ice cover diminished.

Summary

The magnetic record of climate change from Caledonia Marsh over the time interval equivalent to OIS stages 2 and most of 3 is a detrital record. The variations in magnetic properties reflect the varying input of fine-grained glacial flour containing fresh magnetite that was superimposed on a more constant flux of coarser grained, weathered sediment from vast areas of unglaciated catchment. The high and nearly constant magnetite content that characterizes sediment deposited between 21 and 16 ka reflects high and nearly constant input of glacial flour during LGM conditions. Sharp changes in magnetite content that characterize sediment deposited between 35 and 21 ka result from repeated advances and retreats of glaciers. These interpretations are corroborated by textures

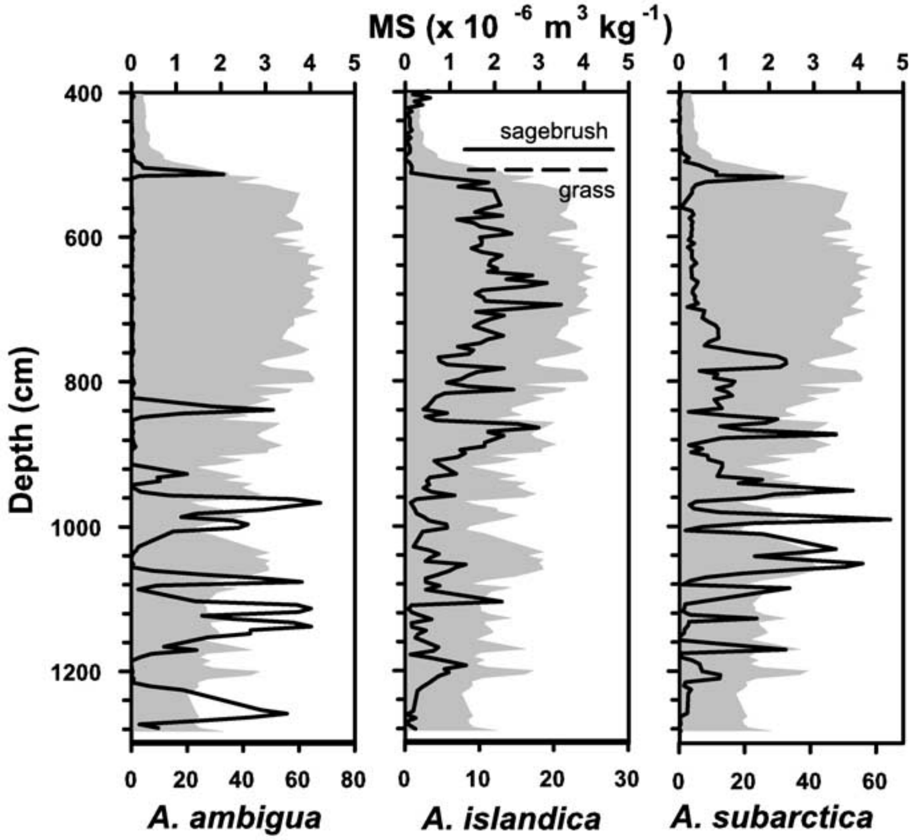

Figure 15. Depth plots of magnetic susceptibility (MS, shaded) with three species of *Aulacoseira* diatoms (see Bradbury et al. 2004b). Sharp declines in sagebrush (grass) pollen begin above solid (dashed) line.

of magnetic particles. Sediment from below about 500 cm depth is characterized by a high proportion of very small (<10 μm), angular particles, and by the presence of abundant unaltered volcanic rock fragments containing fresh magnetite. Sediment from shallower depths is characterized instead by larger (typically 20–100 μm), rounded particles and an absence of fresh volcanic rock fragments. The shape and size features of the particles from deeper than 500 cm in core CM2 closely resemble those of magnetic particles separated from sediment in modern rivers transporting glacial flour (Reynolds et al. 1996).

The large shifts in magnetic, chemical, and textural properties that correspond to deglaciation in the catchment results from several processes. The abrupt decline in magnetite content and iron oxide freshness beginning at about 16 ka reflects the shutdown in glacial flour production. Gradual upward decreases in hematite and elemental contents (e.g., Ti) reflect a gradual buildup in biogenic components and the onset of sediment starvation as marshes clogged the mouths of rivers.

The magnetic results provide a high-resolution record of glacial activity for the southern Cascade Range, showing millennial-scale pulses of glacial-flour input during OIS 3 and mostly constant input during OIS 2. Such a detailed glacial record for western North America contributes to our understanding of global climate change, in particular sub-Milankovitch-scale climate change, its geographic and environmental scope, and the sensitivity by which it may be recorded by alpine glacial sediments deposited in lakes.

Acknowledgements

We are deeply grateful for laboratory analyses and assistance provided by W. Rivers, E. Fisher,

G. Skipp, F. Luiszer, and J. Drexler. Excellent reviews by R. Forester, J. Hagstrum, and C. Geiss are greatly appreciated. We gratefully acknowledge the use of the vibrating sample magnetometer at the Institute for Rock Magnetism, which is funded by the W.M. Keck Foundation, the National Science Foundation, and the University of Minnesota. This work was supported by the Earth Surface Dynamics Program of the US Geological Survey.

References

Adam D.P., Bradbury J.P., Carter C., Dean W.E., Hakala K., McGann M., Reynolds R.L., Rieck H.J., Roberts A.P., Rosenbaum J.G., Sarna-Wojcicki A.M., Schiller K. and Whitlock C. 1995. Status report on cores taken in 1991–1992 in the Upper Klamath Basin and vicinity, Oregon and California. In: Adam D.P., Bradbury J.P., Dean W.E., Gardner J.V. and Sarna-Wojcicki A.M. (eds), Report of the 1994 Workshop on the Correlation of Marine and Terrestrial Records of Climate Changes in the Western United States. US Geological Survey Open-file Report 95-34, pp. 13–29.

Bacon C.R. 1983. Eruptive history of Mount Mazama and Crater Lake caldera, Cascade Range, USA. J. Volcanol. Geothermal Res. 18: 57–115.

Bacon C.R., Lanphere M.A. and Champion D.E. 1999. Late Quaternary slip rate and seismic hazards of the West Klamath Fault zone near Crater Lake, Oregon Cascades. Geology 27: 43–46.

Benson L.V., Burdett J.W., Kashgarian M., Lund S.P., Phillips F.M. and Rye R.O. 1996. Climatic and hydrologic oscillations in the Owens Lake basin and adjacent Sierra Nevada, California. Science 274: 746–749.

Benson L.V. and Thompson R.S. 1987. Lake-level variation in the Lahontan Basin for the past 50,000 years. Quaternary Res. 28: 69–85.

Bischoff J.L., Fitts J.P. and Fitzpatrick J.A. 1997. Responses of sediment geochemistry to climate change in Owens Lake sediment: An 800-k.y. record of saline/fiesh cycles in core OL-92. In: Smith G.I. and Bischoff J.L. (eds), An 800,000-Year Paleoclimate Record From core OL-92, Owens Lake, Southeast California. Geological Society of America, Special Paper 317, pp. 37–47.

Bradbury J.P. 1991. The late Cenozoic diatom stratigraphy and paleolimnology of Tule Lake, Siskiyou Co., California. J. Paleolimnol. 6: 205–255.

Bradbury J.P., Colman S.M. and Reynolds R.L. 2004a. The history of recent Limnological changes and human impact on Upper Klamath Lake, Oregon. J. Paleolim. 31: 151–165 (this issue).

Bradbury J.P., Colman S.M. and Dean W.E. 2004b. Limnological and climatic environments at Upper Klamath Lake, Oregon during the past 45,000 years. J. Paleolim. 31: 167–188 (this issue).

Carver G.A. 1972. Glacial geology of the Mountain Lakes Wilderness and adjacent parts of the Cascade Range. PhD dissertation, University of Washington Oregon. Seattle, 76 pp.

Colman S.M., Bradbury J.P., McGeehin J.P., Holmes C.W., Edginton D. and Sarna-Wojcicki A.M. 2004. Chronology of sediment deposition in Upper Klamath Lake, Oregon. J. Paleolim. 31: 139–149 (this issue).

Colman S.M., Rosenbaum J.G., Reynolds R.L. and Sarna-Wojcicki A.M. 2000. Post-Mazama (7 ka) faulting beneath Upper Klamath Lake, Oregon. Bull. Seismological Soc. Am. 90: 243–247.

Drewry D. 1986. Glacial Geologic Processes. Edward Arnold, London, 276 pp.

Kerwin M.W. 1996. A regional stratigraphic isochron (ca. 8000 ^{14}C yr B.P.) from final deglaciation of Hudson Strait. Quaternary Res. 46: 89–98.

Lovley D.R., Stolz J.F., Nord G.L.Jr. and Phillips E.J.P. 1987. Anaerobic production of magnetite by a dissimilatory iron-reducing microorganism. Nature 330: 252–254.

McKee E.H., Duffield W.A. and Stern R.J. 1983. Late Miocene and early Pliocene basaltic rocks and their implications for crustal structure, northeastern California and south-central Oregon. Geol. Soc. Am. 94: 292–302.

Mortlach R.A. and Froelich P.N. 1989. A simple method for the rapid determination of biogenic opal in pelagic marine sediments. Deep-Sea Res. 36: 1415–1424.

Muhs D.R. 1983. Airborne dust fall on the California Channel Islands, USA. J. Arid Environ. 6: 223–238.

Muhs D.R., Bush C.A., Stewart K.C., Rowland T.R. and Crittenden R.D. 1990. Geochemical evidence of Saharan dust parent material for soils developed on Quaternary limestones of Caribbean and western Atlantic islands. Quaternary Res. 33: 157–177.

Oviatt C.G. 1997. Lake Bonneville fluctuations and global climate change. Geology 25: 155–158.

Petersen N., Von Dobonek T. and Vali H. 1986. Fossil bacterial magnetite in deep-sea sediments from the South Atlantic Ocean. Nature 320: 611–615.

Prentice I.C. 1986. Vegetation responses to past climatic variation. Vegetatio 67: 131–141.

Reynolds R.L., Belnap J. and Reheis M.C. 2001. Aeolian dust in Colorado Plateau soils: Nutrient inputs and recent change in source. Proc. Natl. Acad. Sci. USA 98: 7123–7127.

Reynolds R.L., Rosenbaum J.G., Bradbury J.P., Best P.J., Adam D.P. and Drexler J. 1996. Late Quaternary glacial history of southern Oregon interpreted from sediment magnetism of Upper Klamath Lake. Abstracts with Program, Geological Society of America 1996 Annual Meeting: A-504.

Reynolds R.L., Rosenbaum J.G., Van Metre P., Tuttle M.L., Callender E. and Goldin A. 1999. Greigite (Fe_3S_4) as an indicator of drought – the 1912–1994 magnetic record from White Rock Lake, Dallas, Texas. J. Paleolimnol. 21: 193–204.

Roberts A.P., Reynolds R.L., Verosub K.L. and Adam D.P. 1996. Environmental magnetic implications of greigite (Fe_3S_4) formation in a 3 m.y. lake sediment record from Butte Valley, northern California. Geophys. Res. Lett. 23: 2859–2862.

Rosenbaum J.G. and Reynolds R.L. 2004a. Record of Late Pleistocene glaciation and deglaciation in the southern Cascade Range: II. Flux of glacial flour in a sediment core from Upper Klamath Lake. J. Paleolim. 31: 235–252 (this issue).

Rosenbaum J.G. and Reynolds R.L. 2004b. Basis for paleoenvironmental interpretation of magnetic properties of sediment from Upper Klamath Lake (Oregon): effects of weathering and mineralogical sorting. J. Paleolim. 31: 253–265 (this issue).

Rosenbaum J.G., Reynolds R.L., Adam D.P., Drexler J., Sarna-Wojcicki A.M. and Whitney G.C. 1996. Record of middle Pleistocene climate change from Buck Lake, Cascade Range, southern Oregon-Evidence from sediment magnetism, trace-element geochemistry, and pollen. Geol. Soc. Am. Bull. 108: 1328–1341.

Rosenbaum J.G., Reynolds R.L., Rapp J., Kerwin M., Drexler J. and Adam D.A. 1997. Sediment magnetic, paleomagnetic, geochemical, and grain size data from lacustrine sediment in a core from Upper Klamath Lake, Oregon. US Geological Survey Open-file Report 97-516, 49 pp.

Sherrod D.R. 1991. Geologic map of a part of the Cascade Range between latitudes 43°–44°, central Oregon. US Geological Survey Miscellaneous Investigation Map I-1891.

Smith J.G. 1988. Geologic map of the Pelican Butte quadrangle, Klamath County, Oregon. US Geological Survey map GQ-1653, scale 1: 62,500.

Smith G.I., Bischoff J.L. and Bradbury J.P. 1997. Synthesis of the paleoclimate record from Owens Lake core OL-92. In: Smith G.I. and Bischoff J.L. (eds), An 800,000-Year Paleoclimate Record from Core OL-92, Owens Lake, Southeast California. Geological Society of America, Special Paper 317, pp. 143–160.

Snowball I.F. 1994. Bacterial magnetite and the magnetic properties of sediments in a Swedish lake. Earth Planetary Sci. Lett. 126: 129–142.

Snowball I.F. and Thompson R. 1990. A stable chemical remanence in Holocene sediments. J. Geophys. Res. 95: 4471–4479.

Stoermer E.F. and Smol J.P. 1999. The Diatoms: Applications for the Environmental and Earth Sciences. Cambridge University Press, Cambridge, 484 pp.

Thompson R. and Oldfield F. 1986. Environmental Magnetism. Allen & Unwin, London, 227 pp.

Verosub K.L. and Roberts A.P. 1995. Environmental magnetism: Past, present, and future. J. Geophys. Res. 100: 2175–2192.

Walker G.W. and MacLeod N.S. 1991. Geologic map of Oregon. US Geological Survey.

Webb T.III 1986. Is vegetation in equilibrium with climate change? How to interpret late-Quaternary pollen data. Vegetatio 67: 75–91.

Winchester J.A. and Floyd P.A. 1977. Geochemical discrimination of different magma series and their differentiation products using immobile elements. Geochem. Geol. 20: 325–343.